

Differences in Whole-Cell and Single-Channel Ion Currents across the Plasma Membrane of Mesophyll Cells from Two Closely Related *Thlaspi* Species

Miguel A. Piñeros* and Leon V. Kochian

United States Plant, Soil, and Nutrition Laboratory, United States Department of Agriculture-Agricultural Research Service, Cornell University, Ithaca, New York 14853

The patch clamp technique was used to study the physiology of ion transport in mesophyll cells from two *Thlaspi* spp. that differ significantly in their physiology. In comparison with *Thlaspi arvense*, *Thlaspi caerulescens* (a heavy metal accumulator) can grow in, tolerate, and accumulate very high levels of certain heavy metals (primarily zinc [Zn] and cadmium) in their leaf cells. The membrane conductance of every *T. arvense* leaf cell was dominated by a slowly activating, time-dependent outward rectifying current (SKOR). In contrast, only 23% of *T. caerulescens* cells showed SKOR activity, whereas the remaining 77% exhibit a rapidly developing instantaneous K^+ outward rectifier (RKOR) current. In contrast to RKOR, the channels underlying the SKOR current were sensitive to changes in the extracellular ion activity. Single-channel recordings indicated the existence of K^+ channel populations with similar unitary conductances, but distinct channel kinetics and regulation. The correlation between these recordings and the whole-cell data indicated that although one type of channel kinetics is preferentially activated in each *Thlaspi* spp., both species have the capability to switch between either type of current. Ion substitution in whole-cell and single-channel experiments indicated that although the SKOR and RKOR channels mediate a net outward K^+ current, they can also allow a significant Zn^{2+} permeation (i.e. influx). In addition, single-channel recordings allowed us to identify an infrequent type of plasma membrane divalent cation channel that also can mediate Zn^{2+} influx. We propose that the different K^+ channel types or channel states may result from and are likely to reflect differences in the cytoplasmic and apoplasmic ionic environment in each species. Thus, the ability to interchangeably switch between different channel states allows each species to constantly adjust to changes in their apoplasmic ionic environment.

Implementation of electrophysiological techniques for studying ion transporters in higher plant cells have broadened our understanding of the mechanisms by which plants absorb major ions, such as K^+ and Ca^{2+} , from soils and translocate them to the shoots. Voltage-dependent K^+ channels are by far the best characterized plasma membrane (PM) ion channels in plant cells, typically dominating the PM conductance as slowly activating outward- and inward-rectifying channels (Maathuis et al., 1997). A significant number of the studies regarding K^+ channels have been conducted primarily in root cells, or highly specialized shoot cells, such as pulvinar motor cells and stomatal guard cells (Schroeder et al., 1994; for review, see Assmann, 1993; MacRobbie, 1997). In addition to these time-dependent K^+ currents, instantaneously activating currents have also been described in a variety of root cells (Roberts and Tester, 1995; White and Lemtiri-Chlieh, 1995; Tyerman et al., 1997; Buschmann et al., 2000). Patch clamp studies have indicated that different root tissues from related plant species often display significant differences in current frequencies and activation kinetics of a par-

ticular K^+ conductance (Roberts and Tester, 1995; Keunecke and Hansen, 2000; Zhang et al., 2002), suggesting anatomical and ion transport differences between different plant cells.

In contrast to root cells, the knowledge regarding the properties and regulation of PM K^+ transport in leaf mesophyll cells is much more limited (Spalding et al., 1992; Li and Assmann, 1993; Spalding and Goldsmith, 1993; Li et al., 1994; Kourie, 1996; Romano et al., 1998; Miedema et al., 2000). In the present work, we used the patch clamp technique to study the properties of the ion channels of leaf mesophyll cells from two plant species, which although closely related, differ significantly in their physiology. *Thlaspi caerulescens*, a heavy metal accumulator, can grow in, tolerate, and accumulate very high levels of certain heavy metals (e.g. zinc [Zn] and cadmium) in leaf cells, in comparison with the related nonaccumulator *Thlaspi arvense* (Chaney, 1993; Brown et al., 1994). Therefore, the mesophyll cell PM transporters from these related plant species have had to adapt to significantly different ionic conditions. Our results suggest that differences in the cytoplasmic and apoplasmic ionic environments results in the activation of different K^+ channels types or channel states. Thus, the ability to interchangeably switch between these states allows each species to constantly adjust to changes in their apoplasmic environment.

* Corresponding author; e-mail map25@cornell.edu; fax 607-255-2459.

Article, publication date, and citation information can be found at www.plantphysiol.org/cgi/doi/10.1104/pp.011932.

RESULTS

Cell Morphology and Electrical Characteristics

Mesophyll cell protoplasts isolated from both *Thlaspi* spp. typically contain chloroplasts distributed close to the PM, with little cytoplasm and a large vacuole. Except that *T. caerulescens* leaf mesophyll cells were slightly larger than *T. arvense* cells (Table I), protoplasts isolated from both species were morphologically indistinguishable. Table I summarizes the electrical characteristics for cells from both species. Measurements of resting membrane electrical potentials (E_m) in leaf tissues using impaling electrodes yielded moderately negative E_m values, which did not differ significantly between the two *Thlaspi* spp. Similarity in E_m values between the two species was also observed in patch clamp experiments with mesophyll protoplasts. However, the protoplast E_m measurements were significantly less negative than those in intact tissue and were close to the electrochemical equilibrium for K^+ (E_{K^+}). This indicates that the protoplasts used in patch clamp recordings were predominantly in a depolarized state, where the membrane conductance was not dominated by the proton pump activity (i.e. P state), but rather by the activity of K^+ channels (K state). The patch clamp recordings revealed interesting differences in the kinetics and frequency of the currents dominating the whole conductance of cells from these two species.

Similarities and Differences in Whole-Cell Current Kinetics and Current Frequencies in the Two *Thlaspi* Spp.

The types of PM currents present in the two *Thlaspi* spp. were initially identified in seal solutions (the solutions used to facilitate a tight seal between the patch pipette and the protoplast surface; see "Materials and Methods"), followed by the replacement of the bath solution with solutions varying in their ionic composition. Upon PM depolarization, the whole-cell conductance of every *T. arvense* cell was dominated by a SKOR (Fig. 1A). Only 23% of *T. caerulescens* cells showed SKOR activity, whereas in the

remaining 77% of the cells the whole-cell conductance was dominated by an instantaneous outward current (RKOR; Fig. 1B). In contrast to RKOR currents that developed rapidly, reaching a steady state within 30 to 40 ms, the SKOR currents developed slowly, reaching a steady state within 1 s. The I/V relationships for these two types of currents for whole-cell measurements reversed near the E_{K^+} , indicating K^+ was the main ion underlying these outward currents (Fig. 1C). There were no significant differences between the RKOR and SKOR current densities recorded in *T. caerulescens* cells, nor between the SKOR current densities recorded from cells from the two species. The kinetic properties of the SKOR current in both species were similar, as shown by the similarity in the time constants for activation (Fig. 1D), which decreased as the voltage increased from -40 mV to more positive potentials. The above observations suggested that the same voltage-dependent channels were responsible for SKOR currents and were at similar densities in the two species. The frequency of a particular type of current (i.e. SKOR and RKOR) recorded for the two *Thlaspi* spp. could not be correlated with either cell size, morphology, or with the type of protoplast isolation protocol employed.

Identification of SKOR and RKOR Currents

The ionic selectivities of the SKOR and RKOR currents were studied further in *T. arvense* and *T. caerulescens* cells. When the extracellular K^+ activity was varied over a wide range of concentrations, the SKOR and RKOR currents activated at more negative membrane potentials as the extracellular K^+ activity was reduced (i.e. in the same direction as changes in E_{K^+} ; Fig. 2, A and B). Holding potentials more negative than the theoretical E_{K^+} did not induce any inward currents in cells where SKOR dominated the whole-cell conductance. In contrast, a detailed analysis of the current-voltage relationships obtained for RKOR revealed a small inward current, as indicated by the inflection of the curve at holding potentials more negative than the reversal potential. This inward cur-

Table I. Electrical characteristics of *Thlaspi* spp. mesophyll cells

Characteristics	<i>T. arvense</i>	<i>T. caerulescens</i>
Cell size (μm)	32 ± 1 ($n = 24$)	37 ± 1 ($n = 30$)
Membrane potential (mV): impalement		
200 μM CaCl_2	-154 ± 9 ($n = 12$)	-144 ± 8 ($n = 12$)
Seal solution	-100 ± 9 ($n = 9$)	-114 ± 14 ($n = 9$)
Membrane potential (mV): patch clamp		
Seal solution	-44 ± 5 ($n = 5$)	-39 ± 3 ($n = 20$)
Specific capacitance ($\mu\text{F cm}^2$)	1.3 ± 0.1 ($n = 11$)	1.5 ± 0.2 ($n = 22$)
Frequency of the dominant outward conductance		
Time dependent (slowly activating, time-dependent outward rectifying current [SKOR])	100% ($n = 24$)	23% ($n = 7$)
Instantaneous (rapidly developing instantaneous K^+ outward rectifier [RKOR])	0%	77% ($n = 23$)

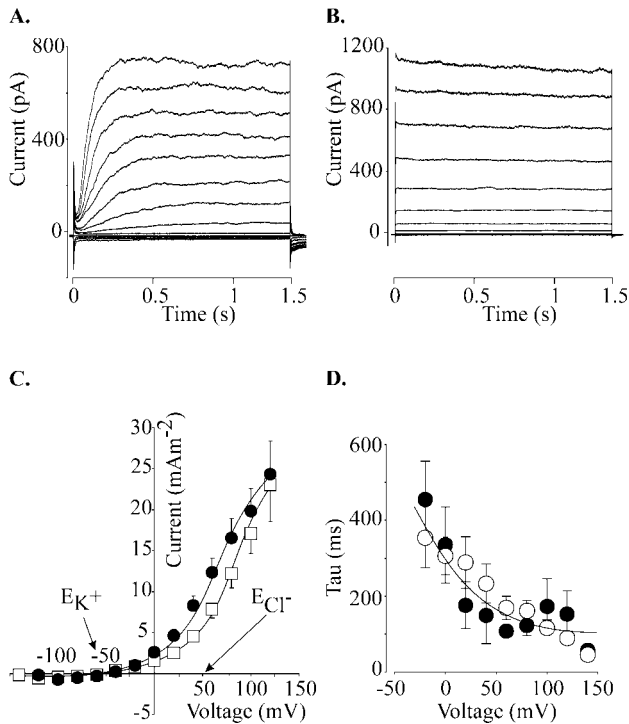


Figure 1. Example of the whole-cell currents measured across the PM of mesophyll protoplasts isolated from *T. arvense* and *T. caerulescens* leaves (see “Materials and Methods” for the detailed explanation of voltage protocols and current measurements). A, SKOR observed in both *Thlaspi* spp. This recording was selected from a representative experiment with *T. arvense*. The diameter of the cell was 33 μm. The bath contained 10 mM K⁺ solution. B, RKOR observed in most *T. caerulescens* cells under identical ionic conditions and voltage protocol as in A. The diameter of the cell was 38 μm. C, Current density-voltage (I/V) relationship of the SKOR (black symbols; n = 21 cells) and RKOR (white symbols; n = 17 cells) derived from currents like those shown in A and B. The data are presented as the average current density (mA m⁻²) to normalize for variations in protoplast surface area values. Error bars denote SE and are not shown for clarity when smaller than the symbol. Arrows indicate the theoretical reversal potentials for K⁺ and Cl⁻ calculated in Table II. D, Comparison of the voltage-dependence for the time constants of activation of the SKOR current estimated from *T. arvense* (black symbols; n = 5) and *T. caerulescens* (white symbols; n = 4) cells (see “Materials and Methods” for detailed explanation).

rent was only evident under ionic conditions where the bath contained high concentrations of KCl (i.e. 50 and 100 mM; Fig. 2B). Deactivation of the SKOR current (i.e. from depolarizing pulses to membrane potentials more negative than the theoretical E_{K⁺}) resulted in small deactivating inward tail currents (Fig. 3A). Analysis of these tail currents established a close relationship between the theoretical E_{K⁺} and the E_{rev} of the SKOR currents (Fig. 3B). Likewise, the E_{rev} of the RKOR current also followed changes in E_{K⁺}. Given that the E_{rev} values obtained for SKOR and RKOR were close to E_{K⁺}, and far from the electrochemical equilibrium potential of any other ion in these solutions (see Table II), K⁺ was the major ion carrying the SKOR and RKOR currents. Neverthe-

less, the E_{rev} values obtained for SKOR and RKOR were consistently less negative than E_{K⁺} as the extracellular K⁺ activity was reduced (Fig. 3B). Such deviations have frequently been attributed to the permeation of the channel by another ionic species with a more positive equilibrium potential (Ca²⁺ or Cl⁻ in the present case). As described later, these deviations were addressed further in single-channel experiments.

Effect of Extracellular Cations on SKOR and RKOR

The sensitivity of the gating of the channels underlying SKOR was further examined by analyzing the voltage dependence of the ionic conductance (Fig. 4A). Under varying extracellular K⁺ conditions, V_{0.5} values became significantly more positive as the extracellular K⁺ activities increased. This suggests that the voltage-dependent gating of the channels underlying SKOR was sensitive to changes in E_{K⁺} or extracellular K⁺. In contrast, the RKOR current was insensitive to changes in extracellular K⁺.

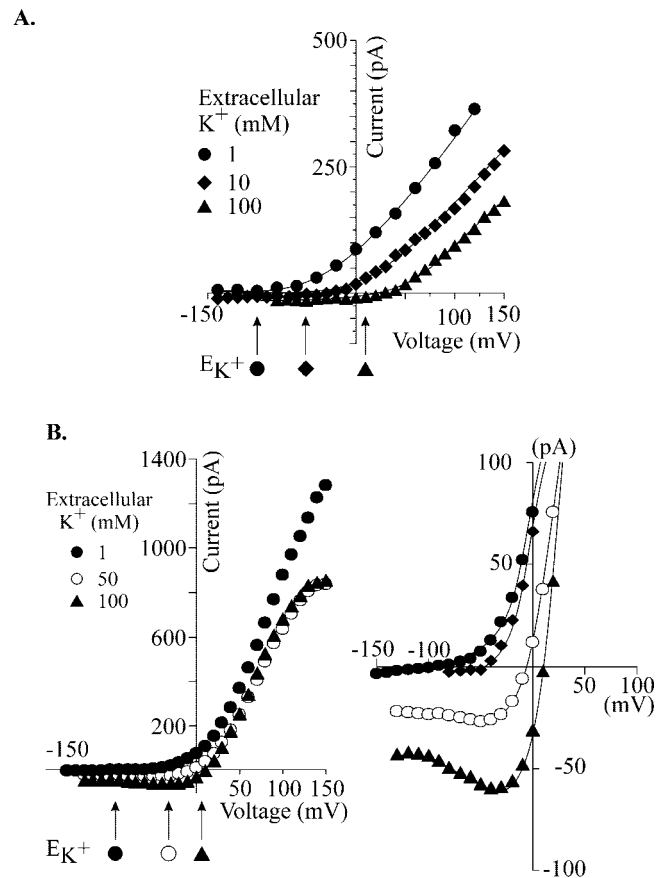


Figure 2. Effect of extracellular K⁺ activity on the SKOR (*T. arvense*; A) and RKOR (*T. caerulescens*; B) currents. The symbols and the arrows below the x axis indicate the calculated E_{K⁺} for each case (see Table II). B, Right, Current-voltage relationships obtained for RKOR at holding potentials near reversal potential (E_{rev}).

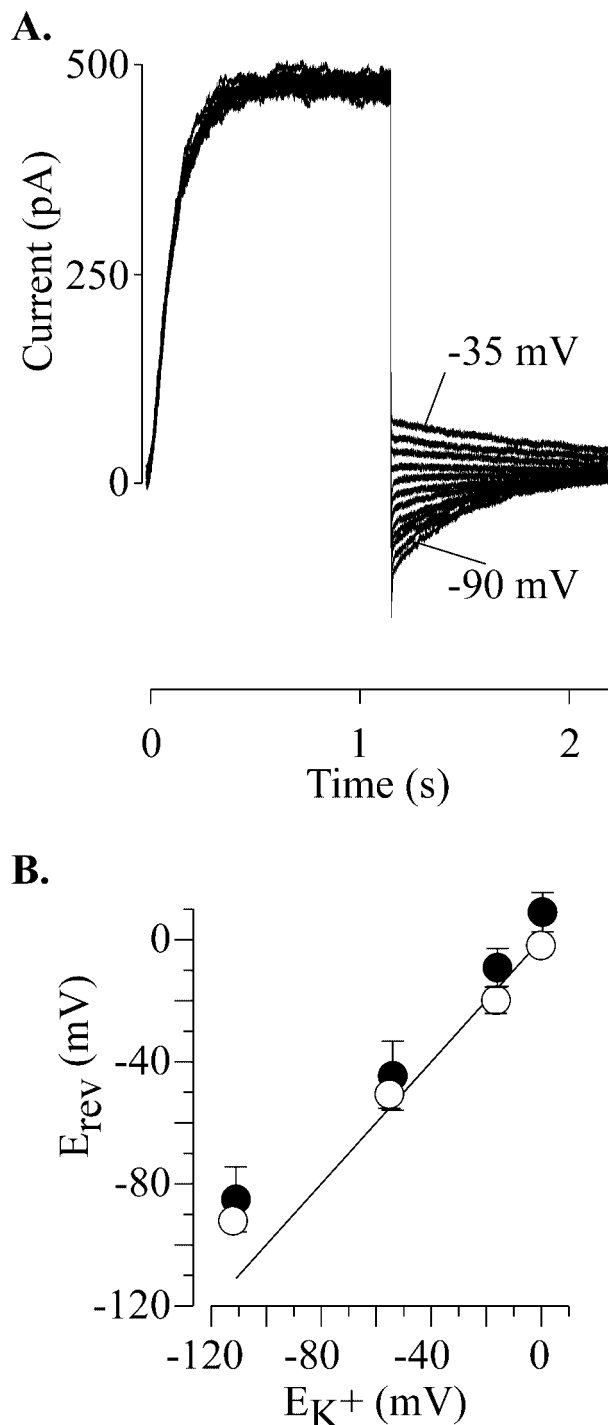


Figure 3. Ion selectivity of the SKOR and RKOR whole-cell currents. A, Example of tail current protocols from SKOR resulting from a voltage step to +60 mV followed by steps to potentials ranging from -90 to -35 mV (in 5-mV steps). The holding potential was -60 mV. B, E_{rev} for SKOR (black symbols) and RKOR (white symbols) plotted as a function of the E_{K^+} (see "Materials and Methods" of details of E_{rev} estimates for each particular current). The line represents values when E_{K^+} equals E_{rev} . E_{K^+} was varied by perfusing the bath with solutions of different K^+ concentrations (see Table II). Each value represents the average of four cells.

Given the large differences in heavy metal accumulation for the two *Thlaspi* spp., we were also interested in examining the effect of Zn^{2+} on the characteristics of both SKOR and RKOR currents. Under the growth conditions imposed in the present study (i.e. 1 μM Zn in the nutrient solution), the Zn concentrations in the leaves of these two *Thlaspi* spp. varied by 10-fold (about 320 and 30 μg Zn g fresh weight⁻¹ in *T. caerulescens* and *T. arvense*, respectively; N. Pence, personal communication), suggesting that in vivo, the mesophyll cells from each species may be exposed to significantly different apoplastic ionic conditions. A concentration-dependent decrease of the SKOR whole-cell conductance was recorded in *T. arvense* protoplasts after the substitution of the K^+ in the bath solution by solutions consisting of different Zn^{2+} activities (Fig. 4, B and C). Exposure to extracellular Zn^{2+} changed the kinetics of outward current from a SKOR-type current (in bath solutions containing K^+) to an RKOR-type current (in bath solutions containing Zn^{2+}). Upon reestablishing the original extracellular K^+ conditions, the magnitude and activation kinetics of the current were partially restored. However, after Zn^{2+} exposure, the outward conductance in 1 mM extracellular K^+ consisted of both SKOR- and RKOR-type currents. The E_{rev} values of the outward currents in the presence of Zn^{2+} were significantly more positive (relative to the extremely negative equilibrium potentials for K^+) and shifted to less negative potentials as the extracellular Zn^{2+} concentration increased. Similar current inhibition, shifts in E_{rev} , and changes in current kinetics upon exposure to extracellular Zn^{2+} were recorded for the SKOR current in *T. caerulescens* protoplasts (data not shown). The effect of extracellular Zn^{2+} on RKOR was examined in *T. caerulescens* cells ($n = 3$; data not shown). Exposure to extracellular Zn^{2+} resulted in a similar current inhibition and shifts in E_{rev} (53 ± 7 , -45 ± 3 , and -30 ± 6 mV in 2, 10, and 50 mM Zn^{2+} , respectively). However, in contrast to SKOR, no change in current kinetics was observed in these cells because the whole-cell conductance was always dominated by the RKOR in extracellular bathing solution containing K^+ or Zn^{2+} (data not shown). Although no inward currents were observed under any of the extracellular Zn^{2+} conditions described above, estimates of $P_{Zn^{2+}}/P_{K^+}$ ranged between 4.5 and 20, with values increasing as the extracellular Zn^{2+} activity decreased.

The effect of extracellular Zn^{2+} on SKOR and RKOR currents was further examined via analysis of the whole-cell conductance-voltage relationships obtained for the various extracellular Zn^{2+} concentrations (Fig. 4D). Although SKOR showed a dependence of $V_{0.5}$ on the extracellular Zn^{2+} concentration similar to that observed for extracellular K^+ , the $V_{0.5}$ values for the RKOR currents were independent of the extracellular ion composition (data not shown). These observations substantiate our previous obser-

Table II. Equilibrium potentials (E_x) for ions in the pipette and bath solutions used in patch clamp recordings of both *Thlaspi* spp.

The pipette solution was constant in all experiments. Equilibrium potentials were calculated from the ionic activities calculated by GEOCHEM-PC. Values are given in mV. >>+ and >>-, Extremely positive and negative, respectively.

Bath Solution	E_K^+	E_{Cl}^-	$E_{Ca^{2+}}$	$E_{Mg^{2+}}$	E_H^+
Seal	-56	29	127	>>-	70
1 mM K^+	-111	84	101	>>-	70
10 mM K^+	-54	51	101	>>-	70
50 mM K^+	-16	16	101	>>-	70
100 mM K^+	0	0	101	>>-	70
2 mM Zn^{2+}	>>+	102	101	>>-	70
10 mM Zn^{2+}	>>+	69	101	>>-	70
50 mM Zn^{2+}	>>+	42	101	>>-	70

vations concerning the sensitivity of the gating of the channels underlying SKOR-type currents to changes in E_K^+ or the extracellular ionic composition.

Single-Channel Recordings

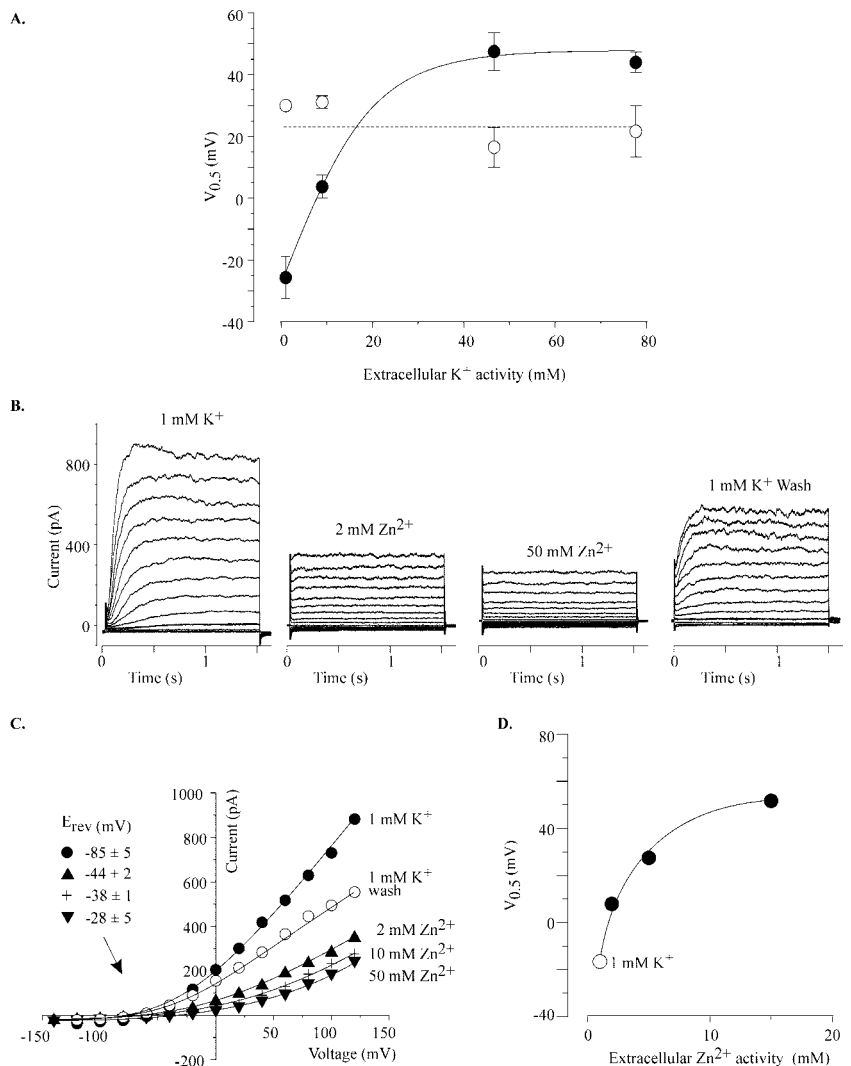
Because single-channel recordings are likely to reflect the differences in the kinetics observed in whole-cell measurements, we recorded single-channel activity in excised outside-out patches isolated from both *Thlaspi* spp. (Fig. 5). However, there were no significant differences in the steady-state kinetics of the single channels recorded from patches isolated from cells displaying the SKOR current in whole-cell configuration and those in patches isolated from cells displaying the RKOR current. Given this lack of correlation, we reconstructed macroscopic currents from single-channel recordings for both species to investigate the source of the different activation kinetics observed in the whole-cell configuration in each species. Summing the single-channel current response from repeated voltage pulse recordings from *T. arvense* patches frequently (four of eight) yielded sigmoidal current curves (Fig. 5C) similar to those observed for SKOR (compare Fig. 5C with Fig. 1, A and D), suggesting that this type of channel underlies the macroscopic SKOR current. However, the remaining four patches yielded curves that resembled the macroscopic RKOR current (data not shown), indicating this type of current can also be present in *T. arvense* cells. Summing single-channel recordings from *T. caerulescens* consistently (five of six) yielded a curve that resembled the predominant RKOR-type current observed in whole-cell preparations from this specie. The remaining patch yielded a macroscopic current similar to the SKOR current described for *T. arvense*. There were no significant differences in unitary conductances and selectivity for K^+ obtained from single-channel recordings from both species (Fig. 6). The E_{rev} for the single-channel current from both species was close to and followed changes in E_K^+ , indicating a high- K^+ selectivity. The single-channel current showed current saturation at about 2.2 pA over the wide range of extracellular K^+ activities tested (Fig. 6, A and B), and an increase in

unitary conductance as the extracellular K^+ activities were increased (Fig. 6D).

We also examined the effect of extracellular Zn^{2+} on the properties of single K^+ channels from *T. arvense*. Increasing the extracellular Zn^{2+} activity resulted in blockade of the single-channel outward K^+ current and caused a positive shift in E_{rev} (Fig. 7). The kinetics of the blockade appeared to be fast, with the time transitions of the blocking and unblocking reactions being too fast to be resolved at the cutoff frequency of the filtering employed, thus appearing as a time-averaged reduction in the single-channel current amplitude. The single-channel blockade by extracellular Zn^{2+} was both concentration and voltage dependent, with the current inhibition being smaller as the holding potentials became more positive. This observation suggests a direct effect of the voltage on the association/dissociation rates of Zn^{2+} binding to a site within the permeation pathway of the channel. In fact, the possibility of Zn^{2+} permeation through these K^+ channels is supported by the high $P_{Zn^{2+}}/P_{K^+}$ values (between 37-70) estimated from the single-channel E_{rev} values. In addition, these observations corroborate that the Zn^{2+} effects recorded in whole-cell experiments result from a direct effect of Zn^{2+} on the outward K^+ channels, and are not solely the product of Zn^{2+} blockade of other permeation pathways.

In two excised patches from *T. caerulescens* (of a total of 25 patches excised in both species), single-channel recordings allowed us to identify an additional and infrequent type of PM channel with different permeation characteristics to those described above for the outward K^+ channel (Fig. 8). In addition to a significantly larger (40 pS) unitary conductance for the outward current, this channel also mediated an inward current (unitary conductance = 14 pS). The single-channel E_{rev} (between -12 and -10 mV) was significantly less negative than that observed for the outward K^+ rectifier (-51 mV) in identical bath solutions. Replacing the bath seal solution with a solution lacking K^+ and containing 10 mM Zn^{2+} did not affect the E_{rev} for this channel nor did this block the outward current (Fig. 8C). In fact,

Figure 4. Effect of extracellular cation activity (K^+ or Zn^{2+}) on SKOR (from *T. arvense*) and RKOR (from *T. caerulea*) currents. A, Gating sensitivity of SKOR ($n = 4$ cells; black symbols) and RKOR ($n = 3$ cells; white symbols) in response to different extracellular K^+ activities. The potential at which the current is half-maximal ($V_{0.5}$) values were estimated as described in "Materials and Methods." Best fittings for $V_{0.5}$ were obtained by setting $\delta = 1$. G_{max} for SKOR and RKOR-type currents remained fairly constant at 2.6 ± 0.4 and 2.8 ± 0.6 nS, respectively, over the entire range of K^+ concentrations. B, Effect of extracellular Zn^{2+} on the whole-cell currents recorded with *T. arvense* protoplasts in 1 mM extracellular K^+ (left) followed by perfusion of the bath with solutions consisting of 2 or 50 mM Zn^{2+} . Extreme right, Whole-cell current after restoring the initial recording conditions. All recordings shown were taken from the same cell. C, I/V relationships for currents shown in B as well as for 10 mM extracellular Zn^{2+} . Data points are from one experiment representative of three independent observations. D, Gating sensitivity of SKOR to extracellular Zn^{2+} activities. $V_{0.5}$ values were derived as in part A from I/V relationships similar to those shown in C. Best fittings for $V_{0.5}$ were obtained by setting $\delta = 1$. G_{max} remained fairly constant (1.8 ± 0.1 nS) over the entire range of Zn^{2+} concentrations. Each $V_{0.5}$ value represents the average of at least three different cells. The $V_{0.5}$ value obtained in 1 mM K^+ before Zn^{2+} exposure is shown for reference (white circle). The curve was drawn for clarity.



under this set of ionic conditions, the unitary conductance of the K^+ outward current increased slightly to 48 pS, whereas a small single-channel inward current (4 pS) could still be detected (Fig. 8, B and C). Allowing for the equilibrium potential of all ions in the solutions, and given the high $P_{Zn^{2+}}/P_{K^+}$ value of 43 (as estimated from the E_{rev}), this small inward current was likely due to Zn^{2+} permeation through this particular channel at depolarizing membrane potentials. Single-channel current-frequency distributions indicated that this type of channel spends more time in the open state as the membrane potential becomes less negative (Fig. 8D). The existence of such a low-frequency and low-conductance PM channel, which opens and allows permeation of a second ionic species (divalent cation) in the same range of membrane potentials where SKOR and RKOR channels activate, could at least partially reconcile the deviations between E_{K^+} and E_{rev} values observed for K^+ conductance in whole-cell recordings.

DISCUSSION

Patch clamp recordings revealed interesting differences between the PM ion transport characteristics of the two *Thlaspi* spp. studied. Although the membrane conductance of every *T. arvense* cell was dominated by the SKOR current, the majority of *T. caerulea* cells displayed RKOR currents. The similarity in current density between cells displaying either type of current indicates that, regardless of the predominant type/state of the current present in each species, their transport limits are similar. The characteristics of the SKOR and RKOR currents in these two *Thlaspi* spp. resemble those reported for cells from the leaf mesophyll (as well as other tissues) from a wide variety of plant species (Table III). Most noticeable, the magnitude of the activation time constants of the SKOR current were very similar to those reported for mesophyll cells from other species (Li and Assmann, 1993; Romano et al., 1998; Miedema et al., 2000). Thus, SKOR and RKOR outward rectifier channels

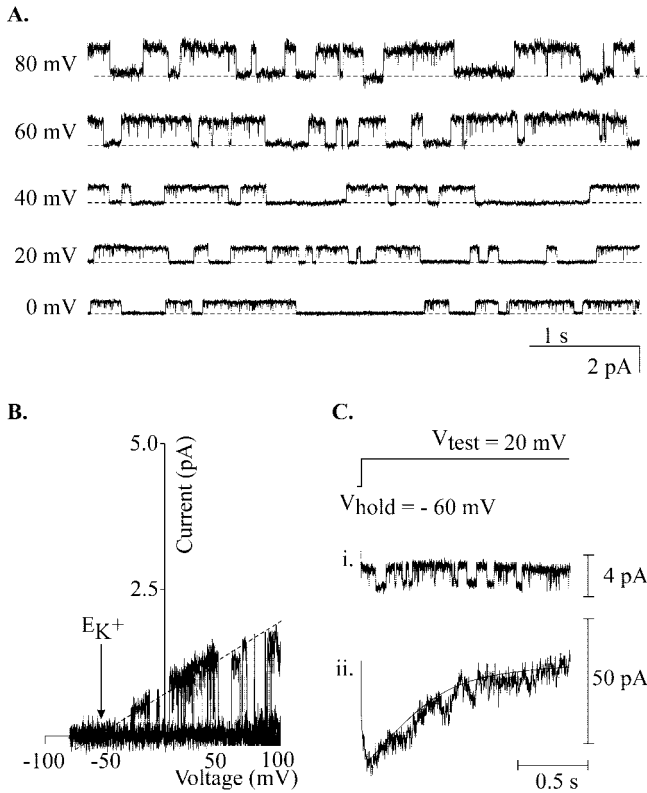


Figure 5. Single K^+ channel recordings from outside out patches from the two *Thlaspi* spp. *A*, Single-channel traces for a patch from a *T. arvense* cell that displayed the SKOR-type current in the whole-cell configuration. The bath contained $10 \text{ mM } K^+$. Membrane potentials were stepped from -60 mV to the voltage indicated in the left margin. The horizontal dashed lines represent the closed state. *B*, Single-channel recordings from an outside out patch from *T. caerulescens* where the RKOR-type current was observed in the whole-cell configuration. The I/V curve was obtained in $10 \text{ mM } K^+$ standard solutions by superimposing six fast ramps after subtracting a ramp in the closed state. The unitary conductance and E_{rev} were 20 pS and -54 mV , respectively (r^2 of 0.985). The arrow indicates the E_{K^+} for these conditions (see Table II). *C*, Time dependence for the activation of the single K^+ channels from *T. arvense* protoplasts. *i*, Single voltage sweep of the K^+ channel activity in an outside-out excised patch in $10 \text{ mM } K^+$ standard solution. *ii*, Macroscopic current reconstruction obtained from the sum of 32 sweeps from the patch in *i* (see “Materials and Methods” for detailed explanation of the reconstruction protocols). The resulting trace was fitted to the same equation applied for macroscopic currents in Figure 1D. The best fit yielded a time constant (λ) of 342 ms .

are likely opened upon membrane depolarization and may play an important role in stabilizing the cell membrane potential (Maathuis et al., 1997). Given their high K^+ selectivity, activation of SKOR and/or RKOR channels at membrane potentials more positive than E_{K^+} would result in a passive K^+ efflux down its electrochemical gradient, allowing the cells to electrically compensate other electrogenic PM transport processes. Variations in PM channel kinetics (i.e. regulation) could potentially speed up or slow down the cell’s response to changes in membrane potential.

The substitution of specific ions in the bathing solution for the whole-cell and single-channel experiments provided insights into the permeation and selectivity properties of the conductance dominating the PM of *Thlaspi* spp. leaf mesophyll cells, first by confirming the K^+ selectivity of the channels underlying the SKOR and RKOR currents. Contrasted with the single-channel observations, the reversal potential of the SKOR and RKOR whole-cell currents departed from E_{K^+} at low extracellular K^+ activities. Such deviations are likely due to permeation by other ionic species contributing to the whole-cell conductance, either via the channels mediating SKOR and

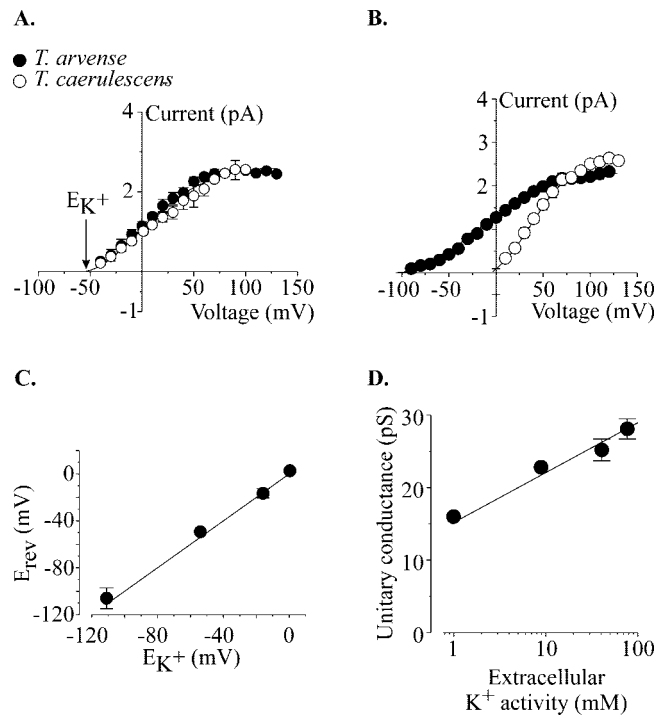


Figure 6. Single-channel characteristics for patches from the two *Thlaspi* spp. *A*, I/V relationship for single-channel recordings similar to those shown in Figure 5 from excised outside out patches from *T. caerulescens* (\circ) and *T. arvense* (\bullet) cells. The bath contained standard $10 \text{ mM } K^+$ solutions. The average unitary conductance and E_{rev} for *T. caerulescens* cells were $20 \pm 1 \text{ pS}$ and -51.1 mV ($n = 5$ patches; $r^2 = 0.993$), and for *T. arvense* were $23 \pm 1 \text{ pS}$ and -49.2 mV ($n = 6$ patches; $r^2 = 0.977$), respectively. The arrow indicates the E_{K^+} shown in Table II. *B*, Effect of changing extracellular K^+ (1 and $100 \text{ mM } K^+$; black and white symbols, respectively) on single-channel current-voltage relationships. Examples are shown for outside out patches excised from *T. arvense* cells. Values are the average of five cells. *C*, Single-channel E_{rev} plotted as a function of the E_{K^+} . E_{K^+} was varied by perfusing the bath solution for *T. arvense* outside-out patches with solutions of varying K^+ concentrations (see Table II). Single-channel E_{rev} values were calculated as described in “Materials and Methods.” Values are the average of five cells. The line represents values when E_{K^+} equals E_{rev} . Similar results were observed in excised patches from *T. caerulescens* (data not shown). *D*, Effect of extracellular K^+ on the single-channel unitary conductance of the K^+ outward rectifier. Unitary conductance values represent an average of at least five different patches from *T. arvense* cells at each concentration.

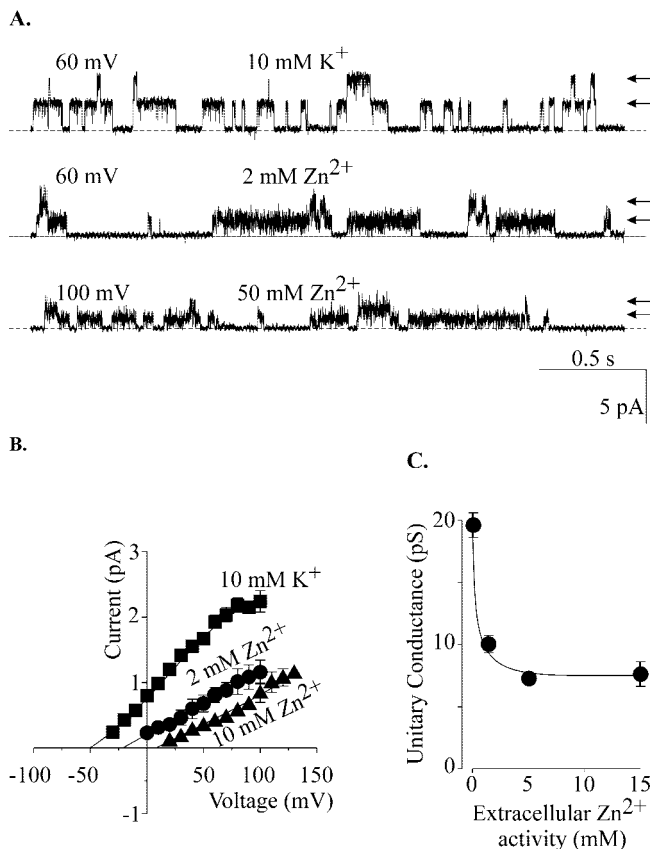


Figure 7. Effect of extracellular Zn^{2+} on the single-channel amplitude and kinetics of the outward K^+ channel. A, Single-channel recordings from an outside-out patch excised from a *T. arvense* protoplast that had displayed the time-dependent-type current in the whole-cell configuration. The bath contained either K^+ or Zn^{2+} at the concentration indicated for each trace. The holding potential is indicated in the left margin of each example trace. The horizontal dashed lines represent the closed state and arrows on the right margin indicate the open states of the two channels observed in this particular example. All traces were from one experiment representative of four independent observations. B, I/V relationships for single channels exposed to bath solution containing either 10 mM K^+ or 2 or 10 mM Zn^{2+} . The E_{rev} shifted from -26 to -2 mV and 4 mV as the Zn^{2+} activities were increased in the bath solution. The I/V relationship for 50 mM Zn^{2+} is not shown for clarity because it resembles that obtained with 10 mM Zn^{2+} . The I/V relationship obtained when the bath contained 10 mM K^+ standard solution is shown for reference. C, Single-channel unitary conductance inhibition as a function of extracellular Zn^{2+} .

RKOR and/or via other types of channels opening at the same range of membrane potentials. Although the gating of SKOR channels was voltage dependent and sensitive to changes in E_{K^+} , RKOR was insensitive to changes in extracellular K^+ and appeared to be fixed at a given voltage. Thus, at high extracellular K^+ , the activation potential of RKOR may be at values more negative than E_{K^+} , therefore allowing the ion influx (i.e. the small inward current) observed in the whole-cell current-voltage relationships. In addition, the relatively large $P_{Zn^{2+}}/P_{K^+}$ values (between 4.5–20) estimated from whole-cell recordings

suggested that although it is too small to be detected as a significant macroscopic inward current, the channel underlying the SKOR and RKOR may in fact have a significant Zn^{2+} permeability. The correlation in changes in current kinetics and current amplitude between the single-channel and whole-cell recordings supports this suggestion.

Exposure of single outward K^+ channels to varying extracellular Zn^{2+} activities resulted in shifts of the current's reversal potential, as well as in channel blockade. The kinetics and the concentration and voltage dependence of the blockade suggests that Zn^{2+} interacts by binding to a site within the channel's permeation pathway. The high $P_{Zn^{2+}}/P_{K^+}$ values (between 37–70) estimated from the single-channel experiments indicate that although these channels mediate a net outward K^+ current, they can also allow a significant Zn^{2+} permeation (i.e. influx). Permeation of divalent cations via PM outward K^+ currents have also been observed for other cell types in a number of plant species and have been suggested to account for similar deviations (Roberts and Tester, 1995, 1997; Zhang et al., 1997; Romano et al., 1998). In addition, we also recorded an infrequent PM channel (Fig. 8) that is active in the same range of membrane potentials where SKOR and RKOR channels activate, allowing a small influx (inward current) of divalent cations (i.e. Ca^{2+} and Zn^{2+}). The activity of such a low-frequency and low-conductance channel allowing influx of other ionic species (i.e. in addition to K^+ fluxes) can also contribute to the observed deviations of E_{rev} from those predicted by ionic activities. The existence, regulation, and permeability (to divalent cations such as Ca^{2+} and heavy metals such as Zn^{2+} and Cd^{2+}) of this particular type of PM channel have already been described previously in root cells from higher plants (Piñeros and Tester, 1997; White et al., 2000).

Varying frequencies of different types of outward K^+ currents has also been reported for other tissues and plant species. For example, although the PM conductance of most maize root stelar cells is dominated by a time-dependent outward K^+ current (with only 20% of the cortical cells displaying this current), this type of current dominates the PM conductance of most cortical cells from wheat (*Triticum aestivum*) roots (Schachtman et al., 1991; Findlay et al., 1994; Roberts and Tester, 1995). In the present study, we were unable to conclusively establish if the two different types of current are the product of two distinct channel populations, or the result of a unique channel population capable of switching between two different kinetic modes. The activation constants for SKOR suggest that the channels underlying this current are likely the same in both species. The correlation between macroscopic currents reconstructed from single-channel recordings and whole-cell recordings indicated that although one type of transporter or state is preferentially activated in each

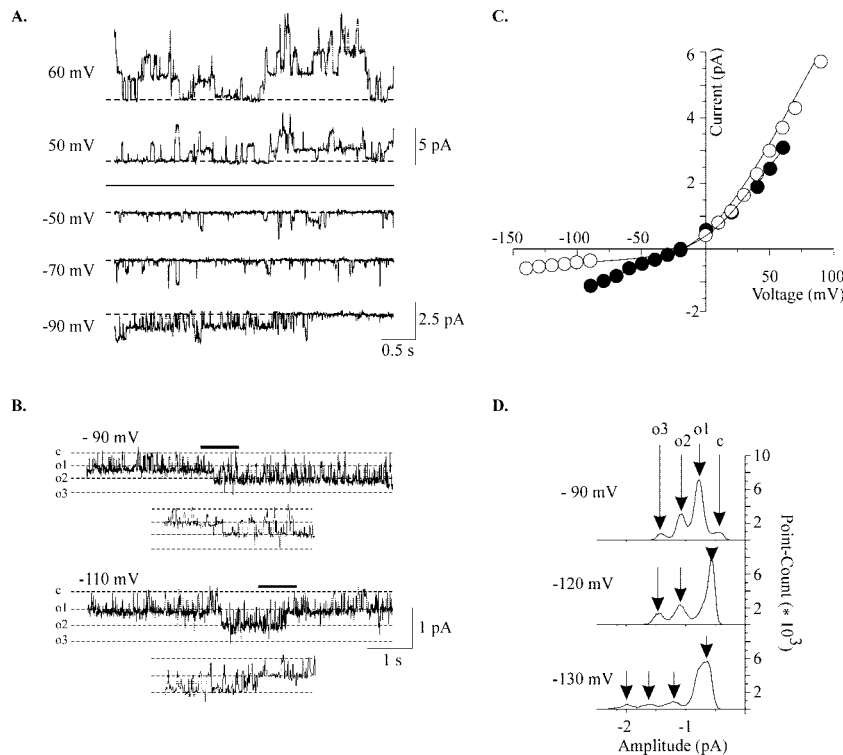


Figure 8. Characteristics of an infrequent PM channel activity mediating both inward and outward currents from an outside-out patch from a *T. caerulescens* protoplast. All traces were taken from one representative experiment. Similar observations were recorded in two isolated patches. A, Representative traces at the holding potentials indicated on the left margin of each trace. Bath solution contained 10 mM CaCl₂ and 10 mM KCl. Dashed line represents the zero current level. Recordings were filtered at 0.5 kHz. B, Representative traces of the inward single-channel currents for the channel described in A after the bath solution was replaced with 10 mM ZnCl₂. The holding potentials are indicated on the left margin of each trace. Dashed line represents the open (o1, o2, and o3) and closed (c) states as indicated on the left of the first traces. The enlargement shown below each trace is for the region marked by the bold line above the trace and is equivalent to a 5-fold expansion of the time scale. Recordings were filtered at 0.1 kHz. C, I/V relationships for the single-channel recordings shown in A (black symbols) and B (white symbols). In Ca²⁺-containing solution (black symbols), the unitary conductances for the outward and inward currents were 40 ± 5 (*r*² = 0.963) and 14.3 ± 1 (*r*² = 0.978) pS and the *E*_{rev} values were -10.4 and -12.4 mV, respectively. In Zn²⁺-containing solution (white symbols), the unitary conductances for the outward and inward current were 48 ± 5 (*r*² = 0.963) and 4 ± 0.1 (*r*² = 0.978) pS and the *E*_{rev} values were -8 and -12 mV, respectively. D, Gaussian curve fitting of the single-channel current-frequency distributions obtained when the bath solution containing 10 mM ZnCl₂. The distributions were generated from 1-min traces (sampling frequency = 2 kHz and bin size = 0.02 pA) obtained at the holding potentials indicated on the left of each set of curves. The arrows on the top of each curve fittings denote the respective closed and open states as shown for the first set of curve fittings.

Thlaspi spp., both species have the transport machinery and ability to activate either type of transporter/state. In fact, although the SKOR current regularly dominated the whole-cell conductance in *T. arvense* cells, occasionally RKOR currents also coexisted in these cells. Furthermore, under particular ionic conditions (i.e. after exposure to extracellular Zn²⁺) the RKOR current could in fact significantly dominate the whole-cell conductance of these cells (see Figs. 1A and 4B). Given the difference in the regulatory characteristics underlying each type of current/state (e.g. sensitivity to changes in the extracellular ionic environment), the ability to switch from one channel type or state to another under particular ionic conditions (e.g. exposure to heavy metals) would allow mesophyll cells to respond to variations in their apoplastic environment.

Under the growing conditions imposed in the present study (i.e. 1 μM Zn), the Zn concentrations in the leaves of these two *Thlaspi* spp. varied by 10-fold. Although epidermal leaf cells in the hyper-accumulator *Thlaspi* spp. accumulate about 4 times more heavy metal than mesophyll cells, the latter can still sequester and tolerate high levels of these metals (Küpper et al., 1999, 2000, 2001). As a consequence, the differences in the cytoplasmic and extracellular ionic environment between the two *Thlaspi* spp. could favor and determine the activation of a particular channel type or state in each species, altering the PM ion transport properties. In the future, it will be of particular interest to evaluate changes in the frequencies of the different types of ion channel currents in mesophyll cells from plants grown under diverse nutrient regimens.

Table III. Current types reported for different tissues and species

Current Type	Tissue	Species	Reference	
SKOR	Cell culture	Tobacco (<i>Nicotiana tabacum</i>)	van Dujin (1993)	
		Guard cells	<i>Vicia faba</i>	Schroeder (1989)
		Mesophyll	Arabidopsis	Romano et al. (1998)
	Roots		<i>V. faba</i>	Miedema et al. (2000)
			Maize (<i>Zea mays</i>)	Li and Assmann (1993)
				Roberts and Tester (1995)
				Piñeros and Kochian (2001)
			<i>Secale cereale</i>	White and Lemtiri-Chlieh (1995)
		Seed coat	<i>V. faba</i>	Zhang et al. (1997)
			<i>Phaseolus vulgaris</i>	Zhang et al. (2000, 2002)
RKOR	Suspension	Maize	Ketchum et al. (1989)	
	Cotyledonary tissue	<i>Amaranthus tricolor</i>	Terry et al. (1992)	
	Roots	Maize (cortex and stele)	Roberts and Tester (1995)	
			Piñeros and Kochian (2001)	
	Seed coats	<i>Hordeum vulgare</i> (parenchyma)	Wegner and De Boer (1997)	
			<i>V. faba</i>	Zhang et al. (1997)
	<i>P. vulgaris</i>	Zhang et al. (2000, 2002)		

The present study clearly shows that the two *Thlaspi* spp. differ significantly in their PM transport characteristics. However, at this time, these differences, which include differences in K⁺ channels as well as Zn²⁺ influx and general divalent cation permeation pathways, cannot be directly related to the mechanism of heavy metal hyperaccumulation in *T. caerulescens*. However, it should be noted that the RKOR, which is found predominantly in *T. caerulescens* leaf mesophyll cells, has the potential to be a significant Zn²⁺ permeation pathway.

Recent studies have started to reveal some of the fundamental mechanisms associated with the metal hyperaccumulation trait in *T. caerulescens* (Lasat et al., 1996, 1998; Pence et al., 2000). Future understanding of the biochemistry of Zn transport across the PM should establish if the K⁺ transport differences observed here play a role in heavy metal hyperaccumulation processes, or are simply a indirect manifestation of some other biochemical or physiological difference between these two species. As our understanding of the function, structure and regulation of mesophyll cell K⁺ transporters increases (Spalding et al., 1992; Li and Assmann, 1993; Spalding and Goldsmith, 1993; Li et al., 1994; Kourie, 1996; Romano et al., 1998; Keuncke and Hansen, 2000; Miedema et al., 2000; Sutton et al., 2000), further elucidation of the regulatory factors and environmental factors affecting ion channels in mesophyll cells should prove illuminating.

MATERIALS AND METHODS

Plant Material

Thlaspi caerulescens ecotype Prayon (provided by Alan J.M. Baker, University of Sheffield, UK) and *Thlaspi arvense* (Crucifer Genetics Cooperative, University of Wisconsin, Madison) seeds were placed in a drop of 0.7% (w/v) low-temperature gelling agarose that sat on nylon mesh circles (1-mm mesh openings), which in turn were positioned on a coarser mesh support covering a 5-L black plastic tub. The nylon mesh was covered with black

polyethylene beads. Seeds were germinated for 5 d in the dark in deionized water. Subsequently, deionized water was replaced with a nutrient solution containing the following macronutrients: Ca, 0.8 mM; K, 1.2 mM; Mg, 0.2 mM; NH₄, 0.1 mM; NO₃, 2.0 mM; PO₄, 0.1 mM; SO₄, 0.2 mM; and micronutrients: BO₃, 12.5 μM; Cl, 50 μM; Cu, 0.5 μM; Fe-N,N'-ethylenebis[2-(2-hydroxyphenyl)-Gly], 10.0 μM; MoO₄, 0.1 μM; Mn, 1.0 μM; Ni, 0.1 μM; and Zn, 1.0 μM. The solution was buffered at pH 5.5 with 1 mM MES-TRIS. Seedlings were grown in a growth chamber at 25°C/15°C (16 h of light and 8 h of dark) under a light intensity of 300 μmol photons m⁻²s⁻¹. Protoplasts were isolated from 2- to 3-week-old plants.

Protoplast Isolation Protocols

Two different protocols for protoplast isolation were employed. The first protocol was a modification of the method described by Elzenga et al. (1991). The abaxial epidermis and midrib of young leaves were removed and the remaining tissue was finely chopped in 5 mL of a solution containing 2 mM CaCl₂, 5 mM MES-KOH (pH 5.5), 0.5% (w/v) polyvinyl pyrrolidone (M_r = 10 000 MW), 0.2% (w/v) bovine serum albumin, 3.4% (w/v) cellulysin (Calbiochem-Novabiochem Co., La Jolla, CA), and 0.026% (w/v) pectolyase (Sigma, St. Louis), and adjusted to 610 mOsm kg⁻¹ with mannitol. The tissue was gently agitated for 5 min, washed and agitated for an additional 5 min in a solution containing 2 mM CaCl₂, 5 mM MES-KOH (pH 5.5), and adjusted to 610 mOsm kg⁻¹ with mannitol. The tissue was then transferred to the patch clamp recording chamber and was placed in a solution containing 10 mM CaCl₂, 10 mM KCl, and 10 mM MES-TRIS (pH 6.0), and adjusted to 210 mOsm kg⁻¹ using sorbitol. Protoplasts from mesophyll tissue swelled and were set free. Protoplasts were allowed to settle and adhere loosely to the glass bottom of the chamber, after which the partially digested tissue was removed by perfusing the chamber with sealing solution (see below). Protoplasts were allowed to osmotically equilibrate for 10 min before attempting to form seals with the patch pipette. The second protocol involved a longer incubation time (1 h at 30°C) in cell wall-digesting enzyme solution, followed by protoplast purification using Suc step gradients. In this protocol the abaxial epidermis and midrib of young leaves were removed, and the protoplasts were isolated from the remaining tissue as described previously (Piñeros and Kochian, 2001). Visual examination of the partially digested tissue, as well as comparisons between protoplasts released by the osmotic shock method and those isolated by longer incubation periods in cell wall-digesting enzymes followed by purification on Suc gradients, confirmed the mesophyll origin of the cells used in patch clamp recordings. In addition, because the morphology of the protoplasts isolated using density gradients were the same, it is likely that protoplasts from the two *Thlaspi* spp. studied here had identical tissue origin.

Recording Solutions

All solutions were filtered (0.22 μm , Millipore, Bedford, MA) before use. The intracellular solutions (pipette filling) consisted of 100 mM KCl, 2 mM MgCl_2 , 10 mM HEPES-TRIS (pH 7.2), 4 mM Na_2ATP , and 2 mM EGTA, and was adjusted to 720 mOsm kg^{-1} using sorbitol. The sealing bathing solution contained 10 mM KCl, 10 mM CaCl_2 , and 10 mM MES-TRIS (pH 6.0). Standard K^+ bath solutions were buffered with 10 mM MES-TRIS (pH 6.0) and contained 1 mM CaCl_2 and KCl to the concentration indicated for each particular case. Bathing solutions containing Zn^{2+} consisted of 10 mM MES-TRIS (pH 6.0) and Zn^{2+} added as ZnCl_2 to the concentration indicated for each particular case. All bath solutions were adjusted to 700 mOsm kg^{-1} using sorbitol.

Electrophysiology

Whole-cell and single-channel currents from excised outside-out patches were recorded with an Axopatch 200A amplifier and a Digitada 1200 data acquisition system (Axon Instruments, Foster City, CA), using the patch clamp technique as described previously (Piñeros and Kochian, 2001). The types of PM currents present in the two *Thlaspi* spp. were initially investigated in seal solution and the bath solution was subsequently replaced by solutions varying in their ionic composition. Whole-cell series resistance and capacitance were partially compensated for by the amplifier. The access resistance was usually less than 20 M Ω . Liquid junction potentials were corrected as described by Neher (1992). E_m was determined from two types of measurements. Membrane potentials were measured in intact leaf sections using an impaling microelectrode. The upper epidermis of a young leaf section was removed gently with fine sandpaper, and the leaf section was positioned in a plexiglas chamber mounted on the stage of a compound microscope. Leaf sections were bathed in 200 μM CaCl_2 (pH 6.0) or in a solution with the same ionic composition as the seal solution used in patch clamp experiments. Leaf sections were allowed to equilibrate for at least 1 h before the impalement was performed. The impaling microelectrode was filled with 3 M KCl (adjusted to pH 2.0 with HCl to reduce tip potentials). The E_m was recorded using a model FD 223 amplifier (World Precision Instruments, Inc., Sarasota, FL) and a single reference electrode. Alternatively, resting potentials were measured from patch clamp experiments, and were recorded as the free-running membrane potential measured immediately after whole-cell seal formation, presumably before perfusion of the protoplast cytoplasm with the pipette solution would take place.

Data Analysis

Patch clamp voltage protocols, current recordings, data storage, and data analysis were done with the software package PClamp 7 (Axon Instruments) and a Pentium III personal computer. Whole-cell data were low-pass filtered at a -3 dB frequency of 2 kHz by the four-pole Bessel filter of the amplifier and digitized at 10 kHz. During whole-cell configuration, the voltage was clamped at a potential equal to the calculated E_{K^+} value (see Table II), and a sequence of voltage pulses stepped in 10- or 20-mV increments (+120 mV to -120 mV) were applied. Between each voltage pulse, there was a 7-s resting phase. The magnitude of the SKOR currents was measured 1 s after imposition of the test potential (i.e. steady state). The E_{rev} values for SKOR were calculated from tail current protocols as follows: Tail current was elicited by stepping the voltage step to +60 mV followed by 12 voltage steps back (in 5 mV at intervals of 15 s) from 30 mV more negative than E_{K^+} to more positive potentials. In between steps, the potential was held at E_{K^+} . The current amplitude of the tail current was calculated immediately after (50 ms) the decay of the capacitance current (amplitude x) and 1 s later, once the currents reached a steady state (amplitude y). The resulting current amplitude from subtracting x from y was plotted against voltage, and the E_{rev} (the potential at which $x - y = 0$) was determined from linear regression.

The E_{rev} values for RKOR were calculated directly from the I/V relationship by a linear regression of the six current amplitude values closest to zero. The activation time constants for the SKOR current were obtained by fitting the currents to a single exponential: $I = I_{\infty} \times \exp(-t/\lambda) + I_1$, where I_{∞} is the amplitude of the steady-state current after activation, λ is the time constant, and I_1 is the steady-state current. The $V_{0.5}$ values from the conductance-voltage relationships analysis were estimated from fittings of the Boltzmann distribution ($G = G_{\text{max}}/[1 + \exp\{-(V_m - V_{0.5})/S\}]$) to con-

ductance (G) to voltage (V) relationships, where G is the chord conductance at a test potential V_m , G_{max} represents the maximum attainable conductance, $V_{0.5}$ represents the potential at which the SKOR or RKOR currents is half-maximal, and S is a slope factor equivalent to $RT/\delta F$, where δ is the minimal gating charge and R, T, and F have their usual meaning. G/V curves (not shown) were derived from I/V relationships according to $G = I_{\text{ss}}/(V_m - E_{\text{rev}})$, where I_{ss} is the steady-state current at the end of the test potential V_m and E_{rev} is the reversal potential of the current. Single-channel data were filtered at 1 kHz and digitized at 10 kHz. Unitary conductance and observed E_{rev} were calculated from the linear regression of the linear portion of the single-channel I/V relationship or the slope of the open state in the case of single-channel ramps (r^2 values are given in parentheses). Macroscopic currents were reconstructed from single-channel recordings were the membrane potential was sweep (stepped from -60 mV to +20 mV) between 30 and 40 times, allowing a 5-s resting phase between sweeps. Capacitive currents were removed by subtracting a sweep where no channel activity was detected from each individual sweep exhibiting channel activity. Subsequently, the reconstructed macroscopic current was obtained by summing the resulting 30 to 40 recordings.

The Nernst potentials for ions in the pipette and bath solutions were calculated using the ionic activities estimated by CHEOCHEM-PC (Parker et al., 1995) and are summarized in Table II. Permeability ratios were calculated using the Fatt and Ginsborg equation (Fatt and Ginsborg, 1958). Error bars denote SE and are not shown when smaller than the symbol.

ACKNOWLEDGMENT

The authors thank Dr. Stephen K. Roberts for his constructive comments on the manuscript.

Received July 27, 2002; returned for revision September 13, 2002; accepted November 6, 2002.

LITERATURE CITED

- Assmann SM (1993) Signal transduction in guard cells. *Annu Rev Cell Biol* 9: 345-375
- Brown SL, Chaney RL, Angle JS, Baker AJM (1994) Phytoremediation potential of *Thlaspi caerulescens* and bladder campion for zinc- and cadmium-contaminated soils. *J Environ Qual* 23: 1151-1157
- Buschmann PH, Vaidyanathan R, Gassmann W, Schroeder JI (2000) Enhancement of Na^+ uptake currents, time dependent inward-rectifying K^+ channel currents, and K^+ channel transcripts by K^+ starvation in wheat root cells. *Plant Physiol* 122: 1387-1397
- Chaney RL (1993) Zinc phytotoxicity. In AD Robson, ed, Zinc in Soil and Plants. Kluwer Academic Publishers, Dordrecht, The Netherlands, pp 135-150
- van Duijn B (1993) Hodgkin-Huxley analysis of whole cell outward rectifying K^+ -currents in protoplast form tobacco cell suspension cultures. *J Membr Biol* 132: 77-85
- Elzenga JTM, Keller CP, VanVolkenburgh E (1991) Patch clamping protoplasts from vascular plants: method for the quick isolation of protoplasts having a high success rate of gigaseal formation. *Plant Physiol* 97: 1573-1575
- Fatt P, Ginsborg BL (1958) The ionic requirements for the production of action potentials in crustacean muscle fibre. *J Phys* 142: 248-255
- Findlay GP, Tyerman SD, Garrill A, Skerret M (1994) Pump and K^+ inward rectifiers in the plasmalemma of wheat root protoplasts. *J Membr Biol* 139: 103-116
- Ketchum KA, Shrier A, Poole RJ (1989) Characterization of potassium-dependent currents in protoplasts of corn suspension cells. *Plant Physiol* 89: 1184-1192
- Keunecke M, Hansen UP (2000) Different pH-dependences of K^+ channel activity in bundle sheath and mesophyll cells of maize leaves. *Planta* 210: 792-800
- Kourie JI (1996) Interaction of extracellular potassium and cesium with the kinetics of inward rectifying K^+ channels in the plasma membrane of mesophyll protoplasts of *Avena sativa*. *Plant Cell Physiol* 37: 770-781
- Küpper H, Lombi E, Zhao FJ, McGrath SP (2000) Cellular compartmentation of cadmium and zinc in relation to other elements in the hyperaccumulator *Arabidopsis halleri*. *Planta* 212: 75-84

- Küpper H, Lombi E, Zhao FJ, Wieshammer G, McGrath SP** (2001) Cellular compartmentation of nickel in the hyperaccumulators *Alyssum lesbiacum*, *Alyssum bertolonii* and *Thlaspi goesingense*. *J Exp Bot* **52**: 2291–2300
- Küpper H, Zhao FJ, McGrath SP** (1999) Cellular compartmentation of zinc in leaves of the hyperaccumulator *Thlaspi caerulescens*. *Plant Physiol* **119**: 305–311
- Lasat MM, Baker AJM, Kochian LV** (1996) Physiological characterization of root Zn²⁺ absorption and translocation to shoots in Zn hyperaccumulator and nonaccumulator species of *Thlaspi*. *Plant Physiol* **112**: 1715–1722
- Lasat MM, Baker AJM, Kochian LV** (1998) Altered Zn compartmentation in the root symplasm and stimulated Zn absorption into the leaf as mechanisms involved in Zn hyperaccumulation in *Thlaspi caerulescens*. *Plant Physiol* **118**: 875–883
- Li W, Assmann SM** (1993) Characterization of a G-protein-regulated outward potassium current in mesophyll cells of *Vicia faba* L. *Proc Natl Acad Sci USA* **90**: 262–266
- Li W, Luan S, Schreiber SL, Assmann SM** (1994) Cyclic AMP stimulates K⁺ channel activity in mesophyll cells of *Vicia faba* L. *Plant Physiol* **106**: 957–961
- Maathuis FJ, Ichida AM, Sanders D, Schroeder JI** (1997) Roles of higher plant K⁺ channels. *Plant Physiol* **114**: 1141–1149
- MacRobbie EAC** (1997) Signaling in guard cells and regulation of ion channel activity. *J Exp Bot* **48**: 515–528
- Miedema H, Romano L, Assmann SM** (2000) Kinetic analysis of the K⁺ selective outward rectifier in *Arabidopsis* mesophyll cells: a comparison with other plant species. *Plant Cell Physiol* **41**: 209–217
- Neher E** (1992) Correction for liquid junction potentials in patch clamp experiments. *Methods Enzymol* **204**: 123–131
- Parker DR, Norvell WA, Chaney RL** (1995) GEOCHEM-PC: a chemical speciation program for IBM and compatible computers. In RH Loeppert, AP Schwab, S Goldberg, eds, *Chemical Equilibrium and Reaction Models*. Soil Science Society of America, Madison, WI, pp 253–269
- Pence NS, Larsen PB, Ebbs SD, Letham DLD, Lasat MM, Garvin DF, Eide D, Kochian LV** (2000) The molecular physiology of heavy metal transporter in the Zn/Cd hyperaccumulator *Thlaspi caerulescens*. *Proc Natl Acad Sci USA* **97**: 4956–4960
- Piñeros MA, Kochian LV** (2001) A patch clamp study on the physiology of aluminum toxicity and aluminum tolerance in maize. Identification and characterization of Al³⁺-induced anion channels. *Plant Physiol* **125**: 292–305
- Piñeros MA, Tester MA** (1997) Calcium channels in higher plant cells: selectivity, regulation and pharmacology. *J Exp Bot* **48**: 551–577
- Roberts SK, Tester M** (1995) Inward and outward K⁺-selective currents in the plasma membrane of protoplasts from maize root cortex and stele. *Plant J* **5**: 811–825
- Roberts SK, Tester M** (1997) Permeation of Ca²⁺ and monovalent cations through and outwardly rectifying channel in maize root stelar cells. *J Exp Bot* **48**: 839–846
- Romano L, Miedema H, Assmann SM** (1998) Ca²⁺ permeable, outwardly-rectifying K⁺ channel in mesophyll cells of *Arabidopsis thaliana*. *Plant Cell Physiol* **39**: 1133–1144
- Schachtman DP, Tyerman SD, Terry BR** (1991) The K⁺/Na⁺ selectivity of a cation channel in the plasma membrane of root cells does not differ in salt-tolerant and salt-sensitive wheat species. *Plant Physiol* **97**: 598–605
- Schroeder JI** (1989) Quantitative analysis of outward rectifying K⁺ channel currents in guard cell protoplasts from *Vicia faba*. *J Membr Biol* **107**: 229–235
- Schroeder JI, Ward JM, Gassmann W** (1994) Perspectives on the physiology and structure of inward rectifying K⁺ channels in higher plants: biophysical implications for K⁺ uptake. *Annu Rev Biophys Biomol Struct* **23**: 441–471
- Spalding EP, Goldsmith MH** (1993) Activation of K⁺ channels in the plasma membrane of *Arabidopsis* by ATP produced photosynthetically. *Plant Cell* **5**: 477–484
- Spalding EP, Slayman CL, Goldsmith MHM, Gradmann D** (1992) Ion channels in *Arabidopsis* plasma membrane. Transport characteristics and involvement in light-induced voltage changes. *Plant Physiol* **99**: 96–102
- Sutton F, Paul SS, Wang XQ, Assmann SM** (2000) Distinct abscisic acid signaling pathways for modulation of guard cells versus mesophyll cell potassium channels revealed by expression studies in *Xenopus laevis* oocytes. *Plant Physiol* **124**: 223–230
- Terry BR, Findlay GP, Tyerman SD** (1992) Direct effects of Ca²⁺-channel blockers on plasma membrane cation channels of *Amaranthus tricolor* protoplasts. *J Exp Bot* **43**: 1457–1473
- Tyerman SD, Skerrett M, Garrill A, Findlay GP, Leith RA** (1997) Pathways for the permeation of Na⁺ and Cl⁻ into protoplasts derived from the cortex of wheat roots. *J Exp Bot* **48**: 459–480
- Wegner LH, De Boer AH** (1997) Properties of two outward-rectifying channels in root xylem parenchyma cells suggest a role in K⁺ homeostasis and long-distance signaling. *Plant Physiol* **115**: 1707–1719
- White PJ, Lemtiri-Chlieh F** (1995) Potassium currents across the plasma membrane of protoplasts derived from rye roots: a patch-clamp study. *J Exp Bot* **286**: 497–511
- White PJ, Piñeros M, Tester M, Ridout M** (2000) Cation permeability and selectivity of a root plasma membrane calcium channel. *J Membr Biol* **174**: 71–83
- Zhang WH, Skerrett M, Walker NA, Patrick JW, Tyerman SD** (2002) Nonselective currents in plasma membrane of protoplasts from coats of developing seeds of bean. *Plant Physiol* **128**: 388–399
- Zhang WH, Walker NA, Tyerman SD, Patrick JW** (1997) Mechanism of solute efflux from seed coats: whole-cell K⁺ currents in transfer cell protoplasts derived from coats of developing seeds of *Vicia faba* L. *J Exp Bot* **313**: 1565–1572
- Zhang WH, Walker NA, Tyerman SD, Patrick JW** (2000) Fast activation of a time-dependent outward current in protoplasts derived from coats of developing *Phaseolus vulgaris* seeds. *Planta* **211**: 894–898